blood®
Regular Article

LYMPHOID NEOPLASIA

Coding and noncoding drivers of mantle cell lymphoma identified through exome and genome sequencing

Prasath Pararajalingam,[1,*] Krysta M. Coyle,[1,*] Sarah E. Arthur,[1] Nicole Thomas,[1] Miguel Alcaide,[1] Barbara Meissner,[2,3] Merrill Boyle,[2,3] Quratulain Qureshi,[1] Bruno M. Grande,[1] Christopher Rushton,[1] Graham W. Slack,[2,3] Andrew J. Mungall,[4] Constantine S. Tam,[5,6] Rishu Agarwal,[5] Sarah-Jane Dawson,[5,6] Georg Lenz,[7] Sriram Balasubramanian,[8] Randy D. Gascoyne,[2,3] Christian Steidl,[2,3] Joseph Connors,[2,3] Diego Villa,[2,3] Timothy E. Audas,[1] Marco A. Marra,[2,3] Nathalie A. Johnson,[9] David W. Scott,[2,3] and Ryan D. Morin[1,4]

[1]Department of Molecular Biology and Biochemistry, Simon Fraser University, Burnaby, BC, Canada; [2]BC Cancer Centre for Lymphoid Cancer and [3]BC Cancer Research Centre, Vancouver, BC, Canada; [4]Michael Smith Genome Sciences Centre, Vancouver, BC, Canada; [5]Peter MacCallum Cancer Centre, Melbourne, VIC, Australia; [6]University of Melbourne, Melbourne, VIC, Australia; [7]Department of Medicine A, Hematology, Oncology, and Pneumology, University Hospital Münster, Münster, Germany; [8]Janssen Research and Development, San Diego, CA; and [9]Department of Medicine, Jewish General Hospital, Montreal, QC, Canada

KEY POINTS

- **RNA-binding proteins with roles in regulating alternative splicing, *DAZAP1*, *EWSR1*, *HNRNPH1*, are frequently mutated in MCL.**
- **Most somatic *HNRNPH1* mutations are intronic and disrupt regulation of HNRNPH1 through alternative splicing.**

Mantle cell lymphoma (MCL) is an uncommon B-cell non-Hodgkin lymphoma (NHL) that is incurable with standard therapies. The genetic drivers of this cancer have not been firmly established, and the features that contribute to differences in clinical course remain limited. To extend our understanding of the biological pathways involved in this malignancy, we performed a large-scale genomic analysis of MCL using data from 51 exomes and 34 genomes alongside previously published exome cohorts. To confirm our findings, we resequenced the genes identified in the exome cohort in 191 MCL tumors, each having clinical follow-up data. We confirmed the prognostic association of *TP53* and *NOTCH1* mutations. Our sequencing revealed novel recurrent noncoding mutations surrounding a single exon of the *HNRNPH1*gene. In RNA-seq data from 103 of these cases, MCL tumors with these mutations had a distinct imbalance of *HNRNPH1* isoforms. This altered splicing of HNRNPH1 was associated with inferior outcomes in MCL and showed a significant increase in protein expression by immunohistochemistry. We describe a functional role for these recurrent noncoding mutations in disrupting an autoregulatory feedback mechanism, thereby deregulating HNRNPH1 protein expression. Taken together, these data strongly imply a role for aberrant regulation of messenger RNA processing in MCL pathobiology. (*Blood*. 2020;136(5):572-584)

Introduction

Mantle cell lymphoma (MCL) is an uncommon B-cell lymphoma representing 4% to 9% of non-Hodgkin lymphoma (NHL) diagnoses worldwide.[1] It can be broadly divided into 2 clinical subtypes, nodal and leukemic nonnodal disease, with each displaying distinct natural history and clinical and genetic features.[2] MCL commonly follows an aggressive clinical course in patients, including nonsustained responses to frontline chemoimmunotherapy and frequent relapses, although some patients, including the majority of those with the leukemic nonnodal variant, exhibit significantly longer survival.[3] Clinical prognostic metrics such as the MCL International Prognostic Index have enabled patient stratification and improvements in frontline therapy, such as the inclusion of active agents (rituximab, bendamustine, and cytarabine) as well as consolidative strategies (autologous stem cell transplantation), have significantly improved outcomes over the past 2 decades.[1,4,5]

The unifying genetic feature of MCL is a chromosomal translocation that places cyclin D1 (*CCND1*) proximal to the immunoglobulin heavy chain enhancer, causing constitutive *CCND1* expression.[2,6] The translocated *CCND1* allele can also accrue secondary mutations including noncoding mutations in the 3′ untranslated region (UTR), thereby enhancing *CCND1* messenger RNA (mRNA) stability and further elevating CCND1 protein abundance.[7,8] Through exome and targeted sequencing efforts, largely focused on nonnodal leukemic subtype, several genes have been identified as commonly mutated in MCL, including those involved in DNA damage response (*ATM*, *TP53*), epigenetic regulation (*KMT2D*, *WHSC1*), Notch signaling (*NOTCH1*, *NOTCH2*), NFκB signaling (*CARD11*, *BIRC3*, *SYK*), and ubiquitin-mediated proteolysis (*UBR5*).[9-11] The genomic features of MCL have proven to be heterogeneous and diverse, and therefore larger comprehensive explorations are necessary to further understand its biological spectrum.

A limited number of recurrent mutations have been associated with prognosis in MCL treated with standard therapy. The most firmly established of these include nonsilent mutations

affecting *TP53*, *NOTCH1*, and *CCND1*,[12-15] as well as amplifications of 3q or deletions in 17p.[13,16] With the ongoing evaluation of new therapeutics for MCL, mutations associated with acquired treatment resistance are beginning to be identified.[17] Despite a broad collection of MCL-related genes and mutations, stratification of patients by proliferation, whereby patients are separated into low-, intermediate-, and high-risk categories, remains more robust than any individual driver mutation.[14,18]

The present study describes driver mutations in MCL and nominates the perturbation of mRNA processing as an important feature of MCL biology. Specifically, we report novel recurrent mutations affecting genes that encode 3 RNA-binding proteins *HNRNPH1*, *DAZAP1*, and *EWSR1*, including intronic mutations affecting exon 4 splicing in *HNRNPH1*. We demonstrate that select mutations in *HNRNPH1* alter this splicing and are associated with higher HNRNPH protein expression in patient tissues. Our functional characterization in MCL patient samples and cell lines indicate that *HNRNPH1* splicing is regulated by the HNRNPH1 protein via a negative feedback loop leading to exclusion of exon 4 in the alternative transcript.

Table 1. Characteristics of patient samples

	Total (n = 213)
Median age (range; n = 189)	64 (31-84)
Male (%)	160/211 (76)
Performance status >1 (%)	35/176 (20)
Blastoid (%)	20/212 (9)
MIPI (%)	
Low	59/138 (43)
Intermediate	34/138 (25)
High	45/138 (33)
Treatment	
R-CHOP	147
Observation	39
Other	5
Unknown	22
HSCT/AUTO	14

MCL tumor samples from 213 patients were obtained from patients living in British Columbia.

MIPI, MCL International Prognostic Index.

Methods

Study design and sequencing

We assembled a discovery cohort of paired fresh-frozen (FF) tumor-normal exome sequencing from 51 novel Canadian cases and 33 previously published cases.[9,11] Our validation cohort consisted of targeted sequencing performed on formalin-fixed, paraffin-embedded tissue representing 191 diagnostic tumor samples from British Columbia (BC) (170 unique cases). Sixteen validation samples and 18 additional FF biopsies from BC underwent whole-genome sequencing (WGS). We performed RNA sequencing (RNA-seq) on a subset of the BC cases (103 total). Patient characteristics are available in Table 1. See supplemental Data and supplemental Figure 1 (available on the *Blood* Web site) for more details. This study was approved by the BC Cancer Research Ethics Board. All participants recruited provided informed consent.

Data analysis

Sequencing reads were aligned to GRCh38 using Burroughs-Wheeler alignment[19] (exomes, WGS), Geneious (targeted), or STAR[20] (RNA-seq; individual-nucleotide resolution crosslinking and immunoprecipitation [iCLIP]). Simple somatic mutations (SSMs) in exomes and WGS were called, by using Strelka (v1.0.14)[21] and Strelka2 (v2.9.6),[22] respectively. Variants were annotated with Variant Effect Predictor[23] using Ensembl release 83 (exomes) and Ensembl release 95 (WGS, targeted). Significantly mutated genes in the discovery cohort were identified by using a voting strategy with results from MutSigCV,[24] OncodriveFM,[25] OncodriveFML,[26] and OncodriveCLUST[27] (false discovery rate [FDR] < 0.1). Targeted sequencing was performed on significantly mutated genes identified by 2 or more methods, as well as *NOTCH1*, *CARD11*, and *NFKBIE*.[11,12,28] Variants from all sequencing approaches were consolidated on a per patient basis. We compared the mutation patterns observed in MCL to diffuse large B-cell lymphoma (DLBCL) by using targeted and exome sequencing data from 1616 unique patients.[29-31]

Experimental approaches

All cell lines were grown as previously described.[12,29] None of the cell lines REC-1, JVM2, Z-138 (in-house sequencing), or HEK cells[32] have *HNRNPH1* mutations at the hot spots identified herein. The HNRNPH1_ex2-6 "minigene" was assembled from human genomic DNA. pEGFP-HNRNPH1 was generated by inserting cDNA encoding the entire open reading frame into the pEGFP-C1 plasmid. Droplet digital polymerase chain reaction (ddPCR), western blot analysis, and tissue microarray immunohistochemistry were performed as described in the supplemental Methods. All ddPCR samples were normalized to the geometric mean of 3 reference genes.

Statistical analysis

Associations between gene mutation status and binary clinical characteristics were assessed, using Fisher's exact test. Overall survival (OS) correlates were separately tested in all patients, regardless of treatment (n = 213), and in the subset of R-CHOP (rituximab, cyclophosphamide, doxorubicin hydrochloride, vincristine, prednisone)–treated, hematopoietic stem cell transplantation–untreated cases (n = 133), using univariate Cox proportional hazard modeling, and *P* values were corrected for multiple-hypothesis testing by the Bonferroni-Hochberg method. Corrected $P < .1$ was considered significant. The *HNRNPH1* exon 4–skipping ratio was derived from RNA-seq data, and survival analysis using this ratio was limited to these cases (n = 102), using the median skipping ratio for all *HNRNPH1*-mutated cases as a cutoff for "mutant-like" splicing. Multivariate survival associations were examined with the Cox proportional hazard model on RNA-seq cases so that the *HNRNPH1* exon 4–skipping ratio could be included in the model

(n = 102). The final tested multivariate model included the *TP53* and *NOTCH1* mutations, *HNRNPH1* mutant-like splicing, and morphology.

Results

Resolving the frequency of SSMs and recurrently mutated genes in MCL

Several genes have previously been implicated as recurrent targets of SSMs in MCL,[9-11,33] although the relevant genes and their mutation incidence has varied considerably among these studies.[34] This variability can be attributed to both genetic heterogeneity in this malignancy and the limited cohort sizes included in each study. To address this problem, we sequenced paired tumor/normal exomes from 51 MCLs diagnosed in Canada and analyzed the data alongside available paired exome data. Three of the 87 available samples exhibited significantly higher mutation burdens (median 5 112; range 1 621-14 959) and were excluded because of the effect of hypermutation on the detection of drivers. In the remaining "discovery cohort," comprising 84 cases, tumor exomes harbored an average of nonsilent SSMs affecting 76 genes (range, 30-219).

Through our analysis of this cohort, 16 genes were deemed recurrently mutated by 2 or more algorithms used to identify driver genes. Three of the algorithms found each of *ATM*, *BIRC3*, *TP53*, *S1PR1*, and *B2M* to be significantly mutated, and each of *MEF2B* and *WHSC1* were identified by 2 methods (supplemental Table 1). Notably, *CCND1*, often affected by somatic hypermutation, was identified by OncodriveCLUST,[27] which relies on spatial clustering of mutations. Of the candidate MCL genes, those frequently mutated were *ATM*, *CCND1*, *TP53*, *WHSC1*, and *KMT2D*, each gene having been previously nominated by other studies. Three genes not previously associated with MCL (*HNRNPH1*, *DAZAP1*, and *EWSR1*) were also identified by at least 2 methods. Each of these 3 genes encode RNA-binding proteins that play a role in regulating RNA maturation, including alternative splicing.[35,36]

Novel mutation patterns in MCL

Based on these results and those of prior studies, we performed targeted sequencing of the coding exons of 18 genes in 191 additional MCLs and separately performed WGS on 34 cases to broadly resolve the exonic and intronic mutation patterns (supplemental Figure 1). We consolidated variants across all samples sequenced by more than one approach and used the resulting nonredundant variants from 272 cases for subsequent analyses. Mutation patterns and prevalence in established MCL genes were largely consistent with prior reports (Figure 1A; supplemental Table 2). Each of *NOTCH1*, *MEF2B*, and *CCND1* have been shown to have mutation hot spots in MCL and other cancers, but the pattern of *MEF2B* mutations in MCL was distinct from that in other cancers (supplemental Figure 2).[7,12,37,38]

Unsurprisingly, the incidence of nonsilent mutations in newly identified genes was generally lower than that in established MCL genes. *EWSR1* was mutated in 8 cases (3%) and *DAZAP1*, in 13 cases (5%; Figure 1A). *EWSR1* predominantly harbored frameshift or nonsense mutations in MCL and exhibited a similar pattern at a lower prevalence in a larger compendium of DLBCLs (0.3%; Figure 1B), suggesting that *EWSR1* has an unappreciated tumor-suppressor function in MCL and possibly in DLBCL. *DAZAP1* had a distinctive pattern, with mutations clustered near the C terminus in a region containing a nuclear localization signal (p.G383-R407)[39] and a proline-rich, protein-binding domain (Figure 1C).[40,41] Nine cases harbored putative truncating mutations, with each predicted to remove or disrupt the nuclear localization signal while leaving most of the open reading frame intact. Nonsynonymous mutations in this region mainly affected highly conserved residues (ie, p.F402, p.R406, and p.R407). Previous work indicates that substitution of these residues causes cytoplasmic accumulation of DAZAP1 in human kidney epithelial (293T) and simian (COS7) cells.[39]

HNRNPH1 intronic mutations disrupt HNRNPH1 binding motifs

HNRNPH1 was mutated in 26 cases (10%) when we consider both coding and noncoding mutations, placing it as the eighth most commonly mutated gene overall (Figure 1A; supplemental Figure 3). Despite limited coverage of introns by our sequencing assay, intronic variants were the most common type of SSM detected in this gene, particularly in the regions surrounding exon 4 (Figure 2A). Paired tumor/normal sequencing confirmed that all recurrent variants were somatic, and the WGS data confirmed that the pattern was restricted to this exon and the immediate flanking regions (Figure 2B). HNRNP proteins are widely involved in regulating splicing by binding to pre-mRNA at specific motifs and either promoting or inhibiting usage of nearby splice sites. Distinct from other HNRNPs, HNRNPH1 (and its paralog HNRNPH2) preferentially binds RNA at poly-G motifs.[42] Strikingly, 73% (19 of 26) of patients with *HNRNPH1* mutations had mutations affecting a poly-G motif within or near this exon. Each of the affected bases are deeply conserved in the homologous region of all available vertebrate genomes, supporting their functional importance.

Further confirming the recurrence of this event, we found mutations in this region of *HNRNPH1* by reanalyzing published and unpublished exomes from 2 recent studies. We observed mutations consistent with the same pattern in 3 of 16 (18.8%) relapsed/refractory MCL exomes sequenced from a recent clinical trial[17] and 4 of 24 (16.7%) exomes from another recent study[43] (supplemental Table 3). We also sequenced this gene in diagnostic tumor tissue from 145 patients treated with either ibrutinib or temsirolimus on a recent clinical trial (clinicaltrials.gov #NCT01646021)[44] and found mutations in 11 (7.5%) of these cases (supplemental Table 3). Among the available WGS data from Burkitt lymphoma[45] (n = 106), DLBCL (n = 153), chronic lymphocytic leukemia (n = 144), and follicular lymphoma (n = 110), we only identified 2 DLBCL patients with *HNRNPH1* mutations in this region (1.3%), suggesting the potential for these to be driver mutations with a highly specific function in MCL biology.[29] This highly reproducible mutation pattern provides strong evidence that these mutations have a regulatory function, most likely affecting the expression and/or splicing of *HNRNPH1* mRNA.

There is a growing list of splicing regulators, including multiple HNRNP family members, that modulate splicing of their mRNA to tightly regulate expression.[46,47] Taking this into consideration along with the prevalence of *HNRNPH1* mutations in sequence contexts resembling HNRNP motifs led us to speculate that HNRNPH1 protein regulates its own expression by modulating the splicing of the *HNRNPH1* transcript. We reanalyzed HNRNPH1 iCLIP-seq data from Uren et al.[42] and confirmed

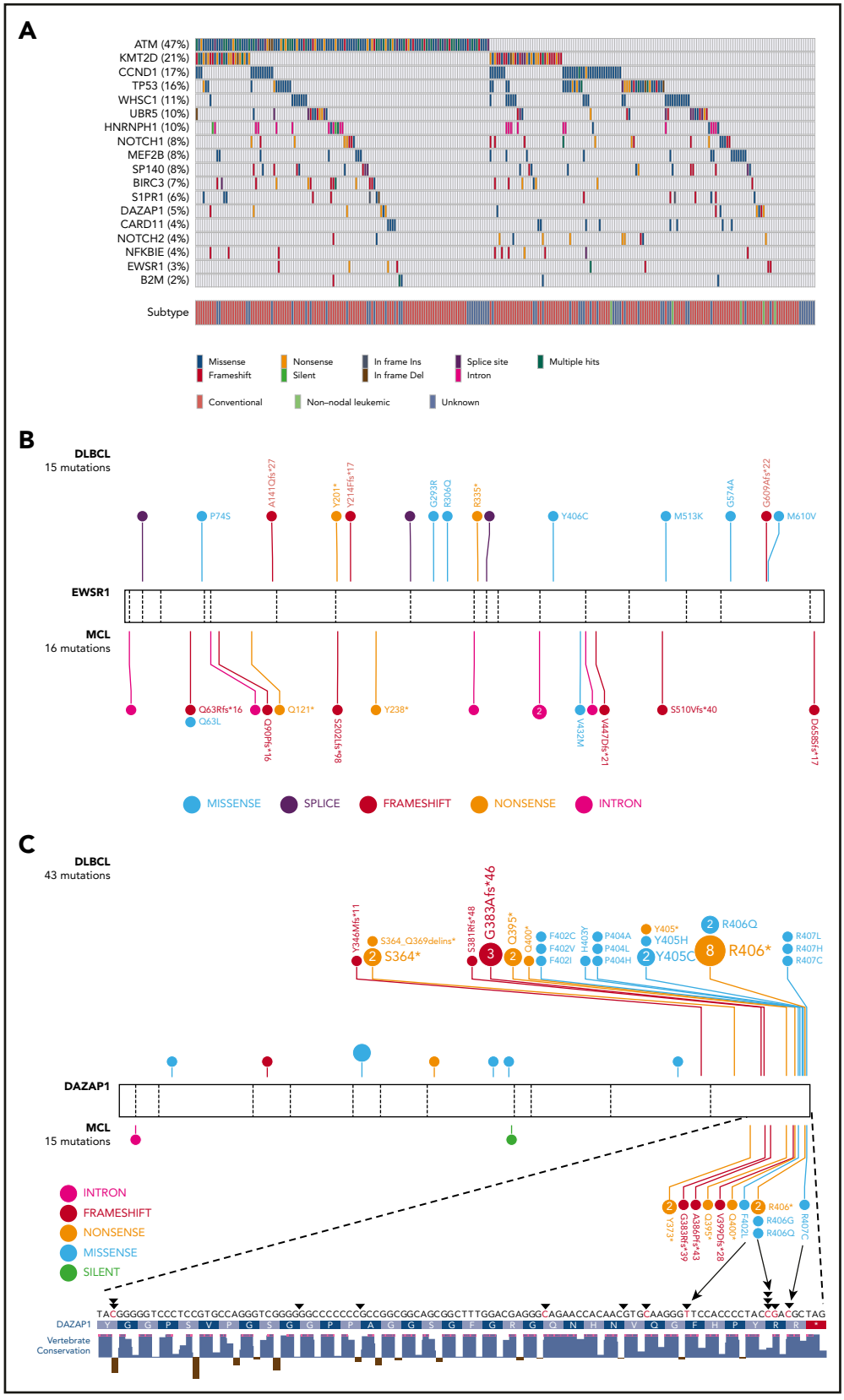

Figure 1. Recurrent mutations are identified in MCL. (A) Mutations observed across 273 MCL samples in 18 candidate MCL genes. Mutations shown here are limited to nonsilent mutations of all genes with the exception of *HNRNPH1*. For this gene, intronic and silent mutations affecting or immediately surrounding exon 4 are included. Spatial distribution of mutations observed in (B) *EWSR1*, and (C) *DAZAP1* in MCL compared with DLBCL.

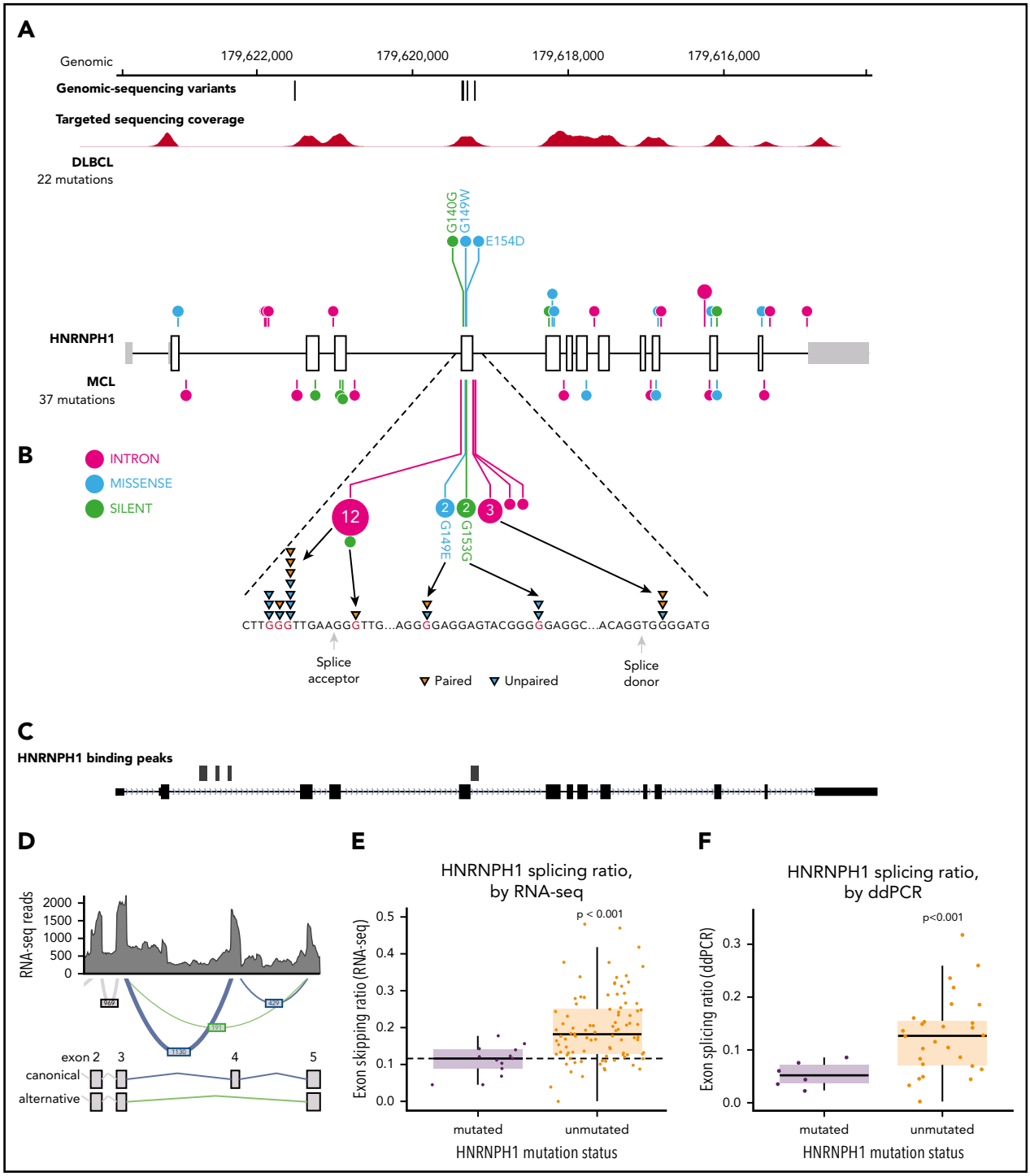

Figure 2. *HNRNPH1* mutations in MCL cluster near exon 4 in poly-G motifs. (A) Somatic mutations found in genomic sequencing cases and targeted sequencing coverage of a representative sample. The prevalence and pattern of mutations in *HNRNPH1* is compared between DLBCL and MCL. (B) Splice site and intronic mutations affecting poly-G motifs were observed both upstream and downstream of exon 4. Paired mutations (orange triangles) are those found to be somatic by sequencing matched constitutional DNA (n = 7). Unpaired mutations (blue triangles) are mutations found in tumor-only DNA sequencing (n = 12). (C) HNRNPH1 iCLIP binding peaks show that HNRNPH1 binds near exon 4 of the transcript (shown is Ref-seq isoform NM_001257293). (D) A representative Sashimi plot of splicing events in *HNRNPH1* are indicated. The canonical splicing events are shown in blue, and the alternative (exon 4 skipping) splice event is shown in green. RNA-seq splicing ratios were calculated by the sum of reads supporting the alternative (green) event, divided by the number of reads supporting the canonical (blue) splicing event. (E) Mutated *HNRNPH1* cases showed significantly lower exon-skipping ratios compared with unmutated cases, as measured by RNA-seq. Cases below the dotted horizontal line (skipping ratio ≤ median mutant skipping ratio) are referred to as mutantlike in further analyses. (F) Digital PCR was used to separately quantify alternative and canonical *HNRNPH1* transcripts in mutant (n = 6) and wild-type (n = 30) cases. Mutant cases exhibit lower rate of exon skipping and higher overall abundance of HNRNPH1 mRNA.

multiple sites of interaction between HNRNPH1 and its pre-mRNA including exon 4 (Figure 2C), supporting a model of direct association at the region affected by mutation.

HNRNPH1 has multiple alternative isoforms including several transcripts that result from skipping of exon 4, which are predicted to be targets of nonsense-mediated decay (NMD) (Figure 2D). Although they do not directly affect canonical splice signals, we hypothesized that the mutations in these poly-G motifs impact the splicing or skipping of exon 4. We analyzed RNA-seq data from 103 cases with known *HNRNPH1* mutation status to evaluate splicing differences between mutated (n = 15) and unmutated (n = 88) tumors. By comparing the number of reads supporting the exon-skipping event to reads supporting inclusion of exon 4, we found that mutated cases exhibited a ratio of isoforms that favors inclusion of exon 4 ($P = 1.13 \times 10^{-5}$, Wilcox rank sum; Figure 2E). We implemented a custom ddPCR assay to separately quantify canonical and alternative *HNRNPH1* transcripts. Using this assay, we corroborated these findings in selected cases ($P < .001$; Figure 2F), which showed a strong correlation ($R = 0.66$; $P < .01$) with splicing ratios determined from RNA-seq data from the corresponding cases (supplemental Figure 4A-B). These results support the notion that *HNRNPH1* mutations favor the inclusion of exon 4, or suppress the skipping of this exon, promoting the formation of the full-length transcript. Based on our model, these mutations disrupt the binding of HNRNPH1 to poly-G motifs surrounding exon 4 and dampen the normal feedback inhibition (supplemental Figure 4C).

HNRNPH1 splicing is associated with inferior outcomes in MCL

We examined whether any mutations identified in this study were associated with patient outcome. This entailed 2 separate analyses: first using all cases with available survival data and then separately, within the subset of cases with R-CHOP treatment. In univariate comparisons, mutations in *NOTCH1* (hazard ratio [HR] = 2.05; $Q = 8.6 \times 10^{-2}$) or *TP53* (HR = 3.38; $Q = 2.8 \times 10^{-7}$) were associated with shorter OS in the complete cohort. Consistent with previous reports, there was also a significant prognostic association of *NOTCH1* (HR = 2.38; $Q = 3.6 \times 10^{-2}$) and *TP53* (HR = 3.53; $Q = 8.4 \times 10^{-6}$) mutations in patients treated with R-CHOP. Notably, although *KMT2D* mutations have been recently implicated as a prognostic feature in MCL,[48] our analysis did not reproduce this result (supplemental Figure 5). In addition, in R-CHOP–treated cases *EWSR1* was associated with shorter OS (HR = 8.71; $Q = 3.5 \times 10^{-3}$), although the number of mutated cases was small. In contrast, a significant association was not observed when these patients were stratified by mutation status of other genes, including HNRNPH1 (supplemental Data). We separately evaluated the effect of *HNRNPH1* mutation status in the relapsed/refractory MCL patients treated with either ibrutinib or temsirolimus. Because of the limited number of mutated cases, patients on both arms of the trial were considered together in this analysis. In contrast to the R-CHOP cohort, patients with *HNRNPH1* mutations had significantly shorter progression-free survival (Figure 3A), providing further support for contribution of these mutations to the biology of MCL.

Given the strong association between *HNRNPH1* alternative splicing and mutation status, we rationalized that the proportion of *HNRNPH1* mRNAs containing exon 4 could be used as a proxy for *HNRNPH1* protein expression. We selected a conservative threshold to assign cases with mutantlike exon skipping based on the median value in all cases with *HNRNPH1* mutations (Figure 2E). In patients with RNA-seq data available (n = 102), this stratification revealed significantly shorter OS in patients with mutantlike splicing of *HNRNPH1* (Figure 3B; HR = 2.50; $P = .00388$). In support of the utility of this information, the splicing ratio was also significantly associated with OS when treated as a continuous variable. In a multivariate analysis, *TP53* mutations, *HNRNPH1* mutant-like splicing, and blastoid morphology were each independently associated with shorter OS (Figure 3C). We conclude that the mutant-like splicing pattern of *HNRNPH1*, which favors the productive isoform, is a novel biomarker of inferior outcome in MCL and is independent of established prognostic genetic features and morphology.

Mutations and alternative splicing influence HNRNPH1 protein expression in MCL

We hypothesized that *HNRNPH1* mutations in poly-G tracts disrupt an autoregulatory negative feedback loop, which predicts a higher HNRNPH protein expression in *HNRNPH1*-mutant tumors. To address this directly, we evaluated HNRNPH expression in 170 MCL tumors by immunohistochemistry (Figure 4A). Of these cases, all had at least 1 type of sequencing data available and 79 had RNA-seq performed. Consistent with our hypothesis, tissues with strong HNRNPH staining intensity were significantly enriched for *HNRNPH1* mutations ($P = .0007214$; Fisher's exact test). Tissues with strong staining were also enriched for cases with mutant-like splicing ($P = .001251$; Fisher's exact test) and the distribution of splicing ratios was significantly different between tissues with moderate and strong staining (Figure 4B). Based on the RNA-seq data, the total mRNA level of *HNRNPH1* was not significantly higher in samples with strong staining (Figure 4C), which suggests that the relative proportion of canonical transcripts, rather than the total mRNA abundance, is more directly related to HNRNPH1 protein expression. Our initial finding showing that an association between productive splicing and survival (Figure 3A) is consistent with the trend observed here: namely, the association between strong HNRNPH staining and shorter survival (Figure 4D).

Common *HNRNPH1* mutations disrupt productive splicing and translation

The correlation between *HNRNPH1* isoform usage and increased protein levels only indirectly implicates NMD in this process. To substantiate the role of NMD in vitro, we inhibited this process by using the eukaryotic translation inhibitor cycloheximide. Cycloheximide is a widely used indirect inhibitor of NMD, owing to the essential role of translation in the NMD process.[49-52] In 3 MCL cell lines (JVM2, REC-1, and Z-138) and in HEK cells, cycloheximide treatment caused a significant and dose-dependent increase in the alternative nonproductive *HNRNPH1* transcript, compared with total *HNRNPH1* transcript (alternative plus canonical; Figure 5A). This was consistent with the change in splicing pattern observed in *SRSF3*, which has alternative isoforms that are targeted to NMD due to inclusion of a poison exon (Figure 5B).[49] These results suggest that the *HNRNPH1* isoforms lacking exon 4 are degraded in an NMD-dependent manner in MCL cells.

To functionally demonstrate that mutations found in MCL disrupt regulation of alternative splicing, we constructed a minigene containing the genomic sequence for *HNRNPH1* from exons 2

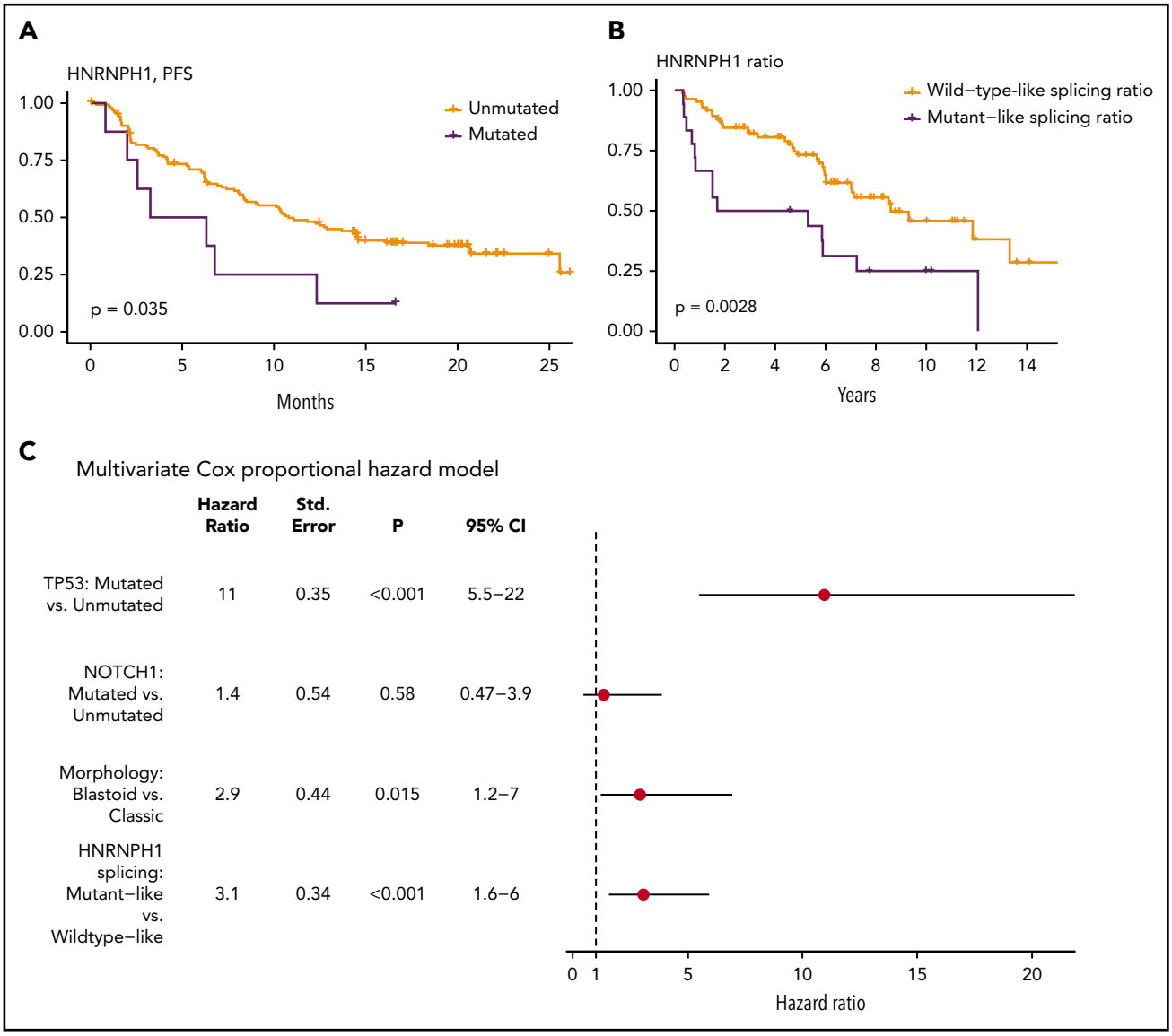

Figure 3. *HNRNPH1* splicing is independently associated with survival in MCL. (A) Survival data and *HNRNPH1* mutation status was obtained for an independent clinical trial cohort (n = 145); cases with *HNRPNH1* mutations exhibit significantly worse progression-free survival (n = 8). (B) All MCL cases with available RNA-seq data (n = 103) were classified as having a mutantlike (n = 18) or wild-type (n = 85) *HNRNPH1* splicing ratio as in Figure 2E, and OS was plotted. Mutantlike *HNRNPH1* splicing was significantly associated with poorer OS. (C) Multivariate Cox proportional modeling was applied to MCL cases with available RNA-seq data (n = 103). TP53 nonsynonymous mutations, *HNRNPH1* mutant-like splicing ratio, and blastoid morphology were independently associated with increased hazard.

through 6 (HNRNPH1_ex2_6), including all intronic sequences. Productive splicing of the minigene created a full-length, in-frame peptide containing the hemagglutinin (HA) tag at the C terminus. Unproductive splicing, resulting from skipping of exon 4, forced the C terminus out of frame and caused translated peptides to lack the terminal HA tag. We first transiently transfected the minigene in HEK cells, along with a vector bearing the cDNA for HNRNPH1 tagged with EGFP. Ectopic expression of HNRNPH1 notably impaired expression of the HA tag, suggesting an HNRNPH1-dependent switch from productive to unproductive splicing of the minigene (Figure 5C). Subsequently, we separately generated 3 distinct mutants of this minigene by site-directed mutagenesis (Figure 5D; Table 2) and transiently transfected each mutant into HEK cells. The presence of any 1 of the 3 mutations tested markedly increased abundance of the HA-tagged peptide, confirming a shift toward productive splicing (Figure 5E). This suggests that all 3 poly-G tracts are individually essential for proper regulation of *HNRNPH1* splicing and adds further support to a model in which these mutations disrupt the autoregulatory feedback cycle and favor HNRNPH1 protein expression (supplemental Figure 4).

Discussion

Using 272 MCL cases, we validated the incidence and pattern of mutations in genes with known relevance to MCL, including *ATM*, *KMT2D*, *TP53*, *CCND1*, and *NOTCH1*. Using clinical data available for the bulk of these cases, we confirmed the prognostic association of mutations in both *TP53* and *NOTCH1*. *NOTCH1* was not independently prognostic in a multivariate model that included *TP53* mutations. We note that in the current data, *WHSC1* mutations were also not associated with OS,

Figure 4. Evaluating HNRNPH expression by tissue microarray. (A) Reactive tonsil tissue stained for HNRNPH expression was used as the reference. Representative images of tumor cores scored as weak (0), moderate (1), or strong (2) HNRNPH staining. (B) Based on the tissues on this tissue microarray with available RNA-seq data (n = 79), higher intensity of HNRNPH staining was associated with a lower splice ratio or a relatively lower proportion of alternative (unproductive transcripts; $P = .01376$, Wilcoxon rank sum). (C) For the same cases as in panel B, cases with higher intensity staining did not have higher levels of HNRNPH1 mRNA based on normalized read counts. In contrast, cases with high-intensity staining were associated with lower HNRNPH1 expression ($P = .02004$; Wilcoxon rank sum). (D) Stratification of patients by moderate or strong HNRNPH staining did not show a significant association with OS, but there was a trend toward inferior outcomes.

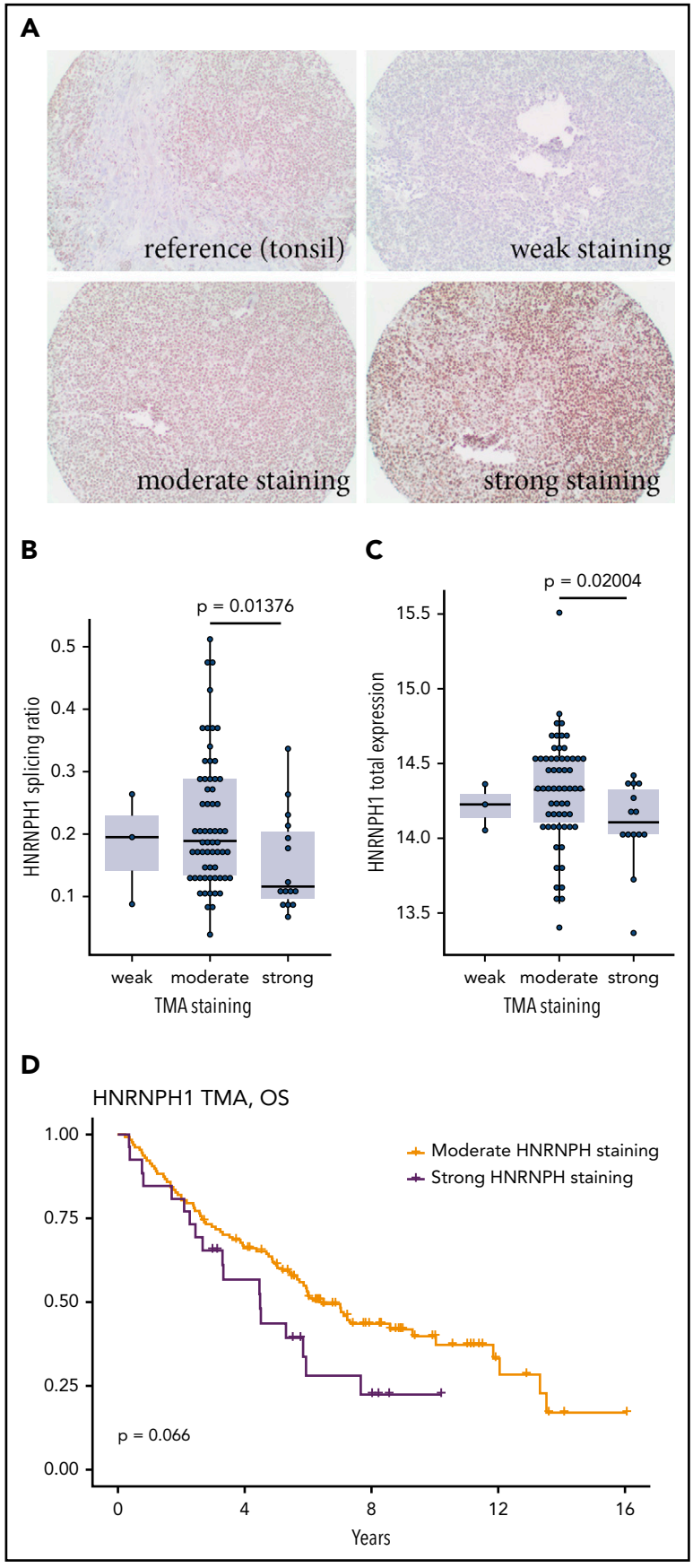

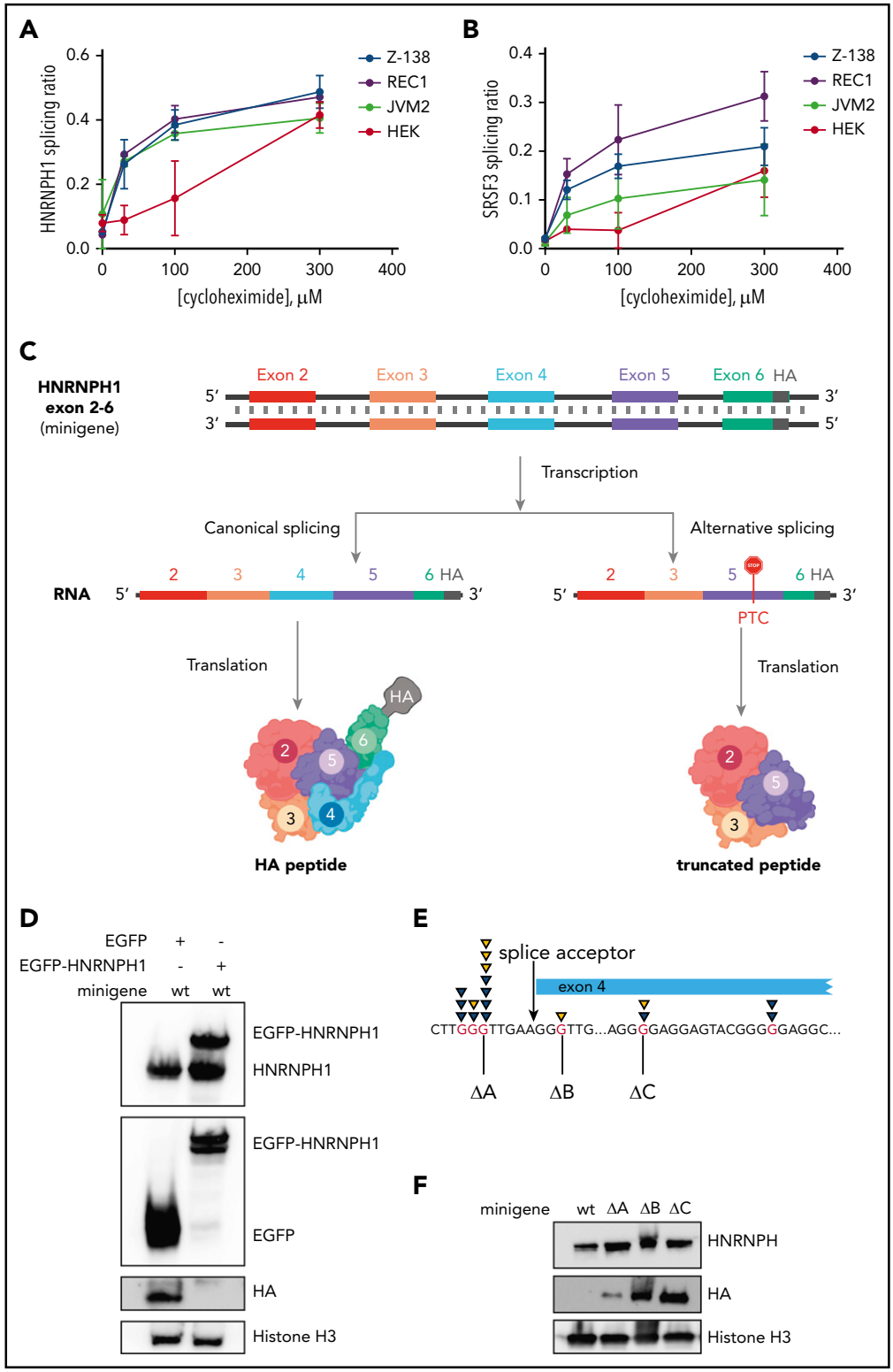

Figure 5. Mutations in HNRNPH1 prevent negative regulation via nonsense-mediated decay. We separately quantified canonical and alternative *HNRNPH1* (A) and *SRSF3* (B) transcripts by digital PCR in MCL cells (REC1, JVM2, and Z138) and HEK cells cultured with cycloheximide (an indirect inhibitor of NMD). This revealed an increasing proportion of the alternative transcript (skipped exon 4 in *HNRNPH1*) with increasing concentrations of cycloheximide. (C) Output from the minigene reporter is represented schematically. Differential splicing of the transcribed pre-mRNA results in inclusion or exclusion of *HNRNPH1* exon 4. The out-of-frame transcript (right) results in the introduction of a premature termination codon (PTC) in exon 5 and translation of a truncated peptide. Translated peptides are represented in cartoon form. (D) HA tag abundance from the wild-type *HNRNPH1* minigene is detected by western blot analysis. HA expression, representing productive splicing, is lost in the presence of HNRNPH1 overexpression. (E) The 3 independent G>T mutations introduced into the *HNRNPH1* minigene are schematically represented in relation to the patient-identified mutations. (F) Expression of the HA tag from wild-type and mutant *HNRNPH1* minigenes are detected by western blot analysis. HA expression, again representing productive splicing, is substantially higher when mutated minigenes are transfected into HEK cells as compared with the wild-type minigene.

Table 2. Specific patient-derived mutations introduced into the *HNRNPH1* minigene

Minigene mutant	Mutation introduced	Corresponding patient mutation	
ΔA	G>T	chr5:179619414 C>A	Intronic
ΔB	G>T	chr5:179619406 C>A	G133G
ΔC	G>A	chr5:179619359 C>T	G149E

Minigene mutations corresponding to patient-identified *HNRNPH1* mutations were introduced.

in contrast to another study,[53] which may be attributable to the limited sample size of that study. Motivated by the putative role of mutations in *HNRNPH1*, we also identified a strong association between HNRNPH1 splicing and outcome. Although the likely consequence of an imbalance of *HNRNPH1* isoforms is an increase in HNRNPH1 protein abundance, we found a stronger association between the splicing ratio and patient outcome. This can be attributed to a limited dynamic range available for scoring HNRNPH expression by immunohistochemistry. In the absence of higher resolution methods for quantifying this protein in tissues, our results indicate that direct measurement of splicing may be a robust biomarker for HNRNPH activity.

Although the incidence was low, we consider the mutation pattern of *EWSR1* to be a notable finding. *EWSR1* is an established cancer gene that is typically discussed in the context of the EWSR1-FLI1 fusion oncoprotein that drives Ewing sarcoma.[54] The pattern of mutations observed here implies a separate tumor-suppressor role of this gene in MCL. Notably, EWSR1 has been implicated in regulating CCND1 by promoting formation of the less oncogenic CCND1a isoform relative to the shorter CCND1b isoform.[55] Although the targets of EWSR1 have not been established in MCL, our data are consistent with the notion that loss of EWSR1 activity alters RNA metabolism and splicing of genes relevant to MCL.

The DAZAP1 mutations described here are similar to previous reports in a subset of DLBCLs.[29,31] The existence of recurrent *EWSR1* and *DAZAP1* mutations in both malignancies add to the limited genetic features shared between DLBCL and MCL, along with inactivating mutations in *KMT2D* and *TP53*. Based on previous mutagenesis experiments,[39] we hypothesize that the more common DAZAP1 mutations cause reduced nuclear occupancy and affect interactions with other proteins, which could disrupt several processes, including transcription, alternative splicing, mRNA transport, and translation.[35,41,56]

Although HNRNPH1 has been identified as overexpressed in other cancer types,[57-59] our description of regulatory mutations in *HNRNPH1* is novel and suggests an unappreciated role for HNRNPH1 in B-cell development and/or lymphomagenesis. HNRNPH1 is a member of the HNRNPH/F family of heterogeneous nuclear ribonucleoproteins[60] and binds to various *cis*-regulatory elements that, depending on the sequence context and interacting proteins, can promote or suppress the use of nearby splice sites.[61] Our data support a model wherein HNRNPH1 protein normally limits its own accumulation by favoring the skipping of exon 4, thus directing its mRNA to NMD. Self-regulation by modulating unproductive splicing, and translation is an emerging theme among other RNA binding proteins, including HNRNPA2B1, HNRNPL, and SRSF3.[46,47,62-64] We have shown, using RNA-seq and ddPCR, that tissues with mutations near exon 4 have a biased representation of the productive isoform containing this exon. The effect of this on protein expression was confirmed through immunohistochemical analysis of tumor tissue. Similar to the predicted effects of other RNA binding proteins with a multiplicity of targets,[65-67] increased expression of HNRNPH1 is expected to have widespread effects on the splicing landscape in MCL.[42,61] The relative paucity of mutations in this region in other B-cell NHL is consistent with a more important role of HNRNPH1 in MCL biology. This warrants further exploration of the suite of genes and splicing events regulated by HNRNPH1 in MCL.

The concurrent identification of 3 novel MCL-related genes (*EWSR1*, *DAZAP1*, and *HNRNPH1*) with related function is compelling, as it may implicate mRNA maturation, splicing, and/or trafficking as a general feature of lymphomagenesis in MCL. Accordingly, there is growing evidence relating alterations in RNA-binding proteins and splice factors in numerous cancers, including other B-cell lymphomas, to various aspects of cancer cell biology.[68-70] Specifically, small changes in RNA-binding proteins can have large downstream effects on gene expression and can thus affect multiple hallmarks of cancer.[71] For example, the splicing factor SF3B1 was identified as recurrently mutated in chronic lymphocytic leukemia,[72-74] and further detailed investigations have identified widespread alternative splicing affecting multiple cellular pathways.[75,76] The identification of pleiotropic effects downstream of SF3B1, including DNA damage response, apoptosis, and Notch signaling, indicate that widespread disruptions to RNA processing can enhance cancer cell survival by multiple pathways.[75,77] Further work will identify these downstream effects in MCL.

In summary, through genomic analysis of 273 MCL tumors, we identified novel recurrently mutated genes with a range of mutation incidences. We implicate an important role for RNA-binding proteins and RNA processing in MCL as compared with other B-cell lymphomas, suggesting that RNA metabolism and splicing have a specific role in MCL pathology. We specifically attribute mutations in *HNRNPH1* to disruptions in HNRNPH1 autoregulation, leading to increased HNRNPH1 protein expression in MCL. Further work that links these mutations to dysregulation of specific RNA molecules will highlight the relevance of RNA processing in MCL.

Acknowledgments

The authors thank Canada's Michael Smith Genome Sciences Centre for library construction, sequencing, and bioinformatics support; Arezoo Mohajeri for the construction of exome libraries; Qiang Pan-Hammarström

for allowing us to use the exome sequencing data from Wu et al[11]; and all patients who provided tissue samples for this study.

This work was supported by the Canadian Institutes of Health Research (CIHR; 300738) and the Terry Fox Research Institute (1021, 1043, and 1061). Some of the biological materials were provided by the Ontario Tumour Bank, which is supported by the Ontario Institute for Cancer Research through funding provided by the Government of Ontario. K.M.C. is supported by a CIHR postdoctoral fellowship.

Authorship

Contribution: P.P. analyzed and interpreted the data; S.E.A. and M.A. performed library preparation; K.M.C. and N.T. analyzed CLIP-seq and RNA-sequencing data; K.M.C. performed cell-based and formalin-fixed, paraffin-embedded tissue–based assays; M.A. performed sequencing and targeted sequencing analysis; B.M.G. provided bioinformatic support and interpreted the data; C.R. analyzed DLBCL mutations; B.M., M.B., G.W.S., A.J.M., and Q.Q. performed nucleic acid extractions and sample quality control; G.W.S. performed tissue microarray scoring; D.V. and D.W.S. provided clinical data and reviewed the cases; D.W.S., T.E.A., M.A.M., N.A.J., R.D.G., C.S., J.C., S.B., S.-J.D., G.L., C.S.T., R.A., and R.D.M. interpreted data, designed the study, and, with P.P. and K.M.C., wrote the manuscript.

Conflict-of-interest disclosure: R.D.G., J.M.C., D.V., and D.W.S. are inventors of the Nanostring nCounter–based MCL35 assay. The remaining authors declare no competing financial interests.

ORCID profiles: P.P., 0000-0003-3945-3552; K.M.C., 0000-0002-1309-4873; B.M.G., 0000-0002-4621-1589; C.R., 0000-0001-6306-9361; A.J.M., 0000-0002-0905-2742; D.V., 0000-0002-4625-3009; T.E.A., 0000-0002-8342-2713; R.D.M., 0000-0003-2932-7800.

Correspondence: Ryan D. Morin, Molecular Biology and Biochemistry, Simon Fraser University, 8888 University Dr, Burnaby, BC V5A 1S6, Canada; e-mail: rdmorin@sfu.ca.

Footnotes

Submitted 9 July 2019; accepted 20 February 2020; prepublished online on *Blood* First Edition 5 March 2020. DOI 10.1182/blood.2019002385.

*P.P. and K.M.C. contributed equally to this work.

All genome and exome data will be submitted to the European Genome-Phenome Archive (EGA) for controlled-access data sharing (accession number EGAS00001004289).

The online version of this article contains a data supplement.

There is a *Blood* Commentary on this article in this issue.

The publication costs of this article were defrayed in part by page charge payment. Therefore, and solely to indicate this fact, this article is hereby marked "advertisement" in accordance with 18 USC section 1734.

REFERENCES

1. Vose JM. Mantle cell lymphoma: 2017 update on diagnosis, risk-stratification, and clinical management. *Am J Hematol*. 2017;92(8):806-813.
2. Chen D, Viswanatha DS, Zent CS, et al. Indolent Mantle Cell Lymphoma: A Distinct Subgroup Characterized by Leukemic Phase Disease without Lymphadenopathy [abstract]. *Blood*. 2009;114(22). Abstract 3937.
3. Abrisqueta P, Scott DW, Slack GW, et al. Observation as the initial management strategy in patients with mantle cell lymphoma. *Ann Oncol*. 2017;28(10):2489-2495.
4. Lim SY, Horsman JM, Hancock BW. The Mantle Cell Lymphoma International Prognostic Index: Does it work in routine practice? *Oncol Lett*. 2010;1(1):187-188.
5. Maddocks K. Update on mantle cell lymphoma. *Blood*. 2018;132(16):1647-1656.
6. Cheah CY, Seymour JF, Wang ML. Mantle Cell Lymphoma. *J Clin Oncol*. 2016;34(11):1256-1269.
7. Mohanty A, Sandoval N, Das M, et al. CCND1 mutations increase protein stability and promote ibrutinib resistance in mantle cell lymphoma. *Oncotarget*. 2016;7(45):73558-73572.
8. Wiestner A, Tehrani M, Chiorazzi M, et al. Point mutations and genomic deletions in CCND1 create stable truncated cyclin D1 mRNAs that are associated with increased proliferation rate and shorter survival. *Blood*. 2007;109(11):4599-4606.
9. Beà S, Valdés-Mas R, Navarro A, et al. Landscape of somatic mutations and clonal evolution in mantle cell lymphoma. *Proc Natl Acad Sci USA*. 2013;110(45):18250-18255.
10. Zhang J, Jima D, Moffitt AB, et al. The genomic landscape of mantle cell lymphoma is related to the epigenetically determined chromatin state of normal B cells. *Blood*. 2014;123(19):2988-2996.
11. Wu C, de Miranda NF, Chen L, et al. Genetic heterogeneity in primary and relapsed mantle cell lymphomas: Impact of recurrent CARD11 mutations. *Oncotarget*. 2016;7(25):38180-38190.
12. Kridel R, Meissner B, Rogic S, et al. Whole transcriptome sequencing reveals recurrent NOTCH1 mutations in mantle cell lymphoma. *Blood*. 2012;119(9):1963-1971.
13. Halldórsdóttir AM, Lundin A, Murray F, et al. Impact of TP53 mutation and 17p deletion in mantle cell lymphoma. *Leukemia*. 2011;25(12):1904-1908.
14. Rosenwald A, Wright G, Wiestner A, et al. The proliferation gene expression signature is a quantitative integrator of oncogenic events that predicts survival in mantle cell lymphoma. *Cancer Cell*. 2003;3(2):185-197.
15. Tam CS, Anderson MA, Pott C, et al. Ibrutinib plus Venetoclax for the Treatment of Mantle-Cell Lymphoma. *N Engl J Med*. 2018;378(13):1211-1223.
16. Espinet B, Salaverria I, Bea S, et al. Incidence and prognostic impact of secondary cytogenetic aberrations in a series of 145 patients with mantle cell lymphoma. *Genes Chromosome Canc*. 49(5):439-451.
17. Agarwal R, Chan Y-C, Tam CS, et al. Dynamic molecular monitoring reveals that SWI-SNF mutations mediate resistance to ibrutinib plus venetoclax in mantle cell lymphoma. *Nat Med*. 2019;25(1):119-129.
18. Scott DW, Abrisqueta P, Wright GW, et al; Lymphoma/Leukemia Molecular Profiling Project. New Molecular Assay for the Proliferation Signature in Mantle Cell Lymphoma Applicable to Formalin-Fixed Paraffin-Embedded Biopsies. *J Clin Oncol*. 2017;35(15):1668-1677.
19. Li H. Aligning sequence reads, clone sequences and assembly contigs with BWA-MEM. *arXiv*. 2013;1303.3997.
20. Dobin A, Davis CA, Schlesinger F, et al. STAR: ultrafast universal RNA-seq aligner. *Bioinformatics*. 2013;29(1):15-21. doi:10.1093/bioinformatics/bts635
21. Saunders CT, Wong WSW, Swamy S, Becq J, Murray LJ, Cheetham RK. Strelka: accurate somatic small-variant calling from sequenced tumor-normal sample pairs. *Bioinformatics*. 2012;28(14):1811-1817.
22. Kim S, Scheffler K, Halpern AL, et al. Strelka2: fast and accurate calling of germline and somatic variants. *Nat Methods*. 2018;15(8):591-594.
23. McLaren W, Gil L, Hunt SE, et al. The Ensembl Variant Effect Predictor. *Genome Biol*. 2016;17(1):122.
24. Lawrence MS, Stojanov P, Polak P, et al. Mutational heterogeneity in cancer and the search for new cancer-associated genes. *Nature*. 2013;499(7457):214-218.
25. Gonzalez-Perez A, Lopez-Bigas N. Functional impact bias reveals cancer drivers. *Nucleic Acids Res*. 2012;40(21):e169.
26. Mularoni L, Sabarinathan R, Deu-Pons J, Gonzalez-Perez A, López-Bigas N. OncodriveFML: a general framework to identify coding and non-coding regions with cancer driver mutations. *Genome Biol*. 2016;17(1):128.
27. Tamborero D, Gonzalez-Perez A, Lopez-Bigas N. OncodriveCLUST: exploiting the positional clustering of somatic mutations to identify cancer genes. *Bioinformatics*. 2013;29(18):2238-2244.

28. Mansouri L, Noerenberg D, Young E, et al. Frequent NFKBIE deletions are associated with poor outcome in primary mediastinal B-cell lymphoma. *Blood*. 2016;128(23): 2666-2670.

29. Arthur SE, Jiang A, Grande BM, et al. Genome-wide discovery of somatic regulatory variants in diffuse large B-cell lymphoma. *Nat Commun*. 2018;9(1):4001.

30. Reddy A, Zhang J, Davis NS, et al. Genetic and Functional Drivers of Diffuse Large B Cell Lymphoma. *Cell*. 2017;171(2): 481-494.e15.

31. Schmitz R, Wright GW, Huang DW, et al. Genetics and Pathogenesis of Diffuse Large B-Cell Lymphoma. *N Engl J Med*. 2018; 378(15):1396-1407.

32. Lin Y-C, Boone M, Meuris L, et al. Genome dynamics of the human embryonic kidney 293 lineage in response to cell biology manipulations. *Nat Commun*. 2014;5(1):4767.

33. Meissner B, Kridel R, Lim RS, et al. The E3 ubiquitin ligase UBR5 is recurrently mutated in mantle cell lymphoma. *Blood*. 2013;121(16): 3161-3164.

34. Ahmed M, Zhang L, Nomie K, Lam L, Wang M. Gene mutations and actionable genetic lesions in mantle cell lymphoma. *Oncotarget*. 2016;7(36):58638-58648.

35. Smith RWP, Anderson RC, Smith JWS, Brook M, Richardson WA, Gray NK. DAZAP1, an RNA-binding protein required for development and spermatogenesis, can regulate mRNA translation. *RNA*. 2011;17(7): 1282-1295.

36. Paronetto MP, Miñana B, Valcárcel J. The Ewing sarcoma protein regulates DNA damage-induced alternative splicing. *Mol Cell*. 2011;43(3):353-368.

37. Fabbri G, Rasi S, Rossi D, et al. Analysis of the chronic lymphocytic leukemia coding genome: role of NOTCH1 mutational activation. *J Exp Med*. 2011;208(7):1389-1401.

38. Morin RD, Mendez-Lago M, Mungall AJ, et al. Frequent mutation of histone-modifying genes in non-Hodgkin lymphoma. *Nature*. 2011;476(7360):298-303.

39. Lin Y-T, Yen PH. A novel nucleocytoplasmic shuttling sequence of DAZAP1, a testis-abundant RNA-binding protein. *RNA*. 2006; 12(8):1486-1493.

40. Dai T, Vera Y, Salido EC, Yen PH. Characterization of the mouse Dazap1 gene encoding an RNA-binding protein that interacts with infertility factors DAZ and DAZL. *BMC Genomics*. 2001;2(1):6.

41. Choudhury R, Roy SG, Tsai YS, Tripathy A, Graves LM, Wang Z. The splicing activator DAZAP1 integrates splicing control into MEK/Erk-regulated cell proliferation and migration. *Nat Commun*. 2014;5(1):3078.

42. Uren PJ, Bahrami-Samani E, de Araujo PR, et al. High-throughput analyses of hnRNP H1 dissects its multi-functional aspect. *RNA Biol*. 2016;13(4):400-411.

43. Khodadoust MS, Olsson N, Wagar LE, et al. Antigen presentation profiling reveals recognition of lymphoma immunoglobulin neoantigens. *Nature*. 2017;543(7647):723-727.

44. Rule S, Jurczak W, Jerkeman M, et al. Ibrutinib versus temsirolimus: 3-year follow-up of patients with previously treated mantle cell lymphoma from the phase 3, international, randomized, open-label RAY study. *Leukemia*. 2018;32(8):1799-1803.

45. Grande BM, Gerhard DS, Jiang A, et al. Genome-wide discovery of somatic coding and noncoding mutations in pediatric endemic and sporadic Burkitt lymphoma. *Blood*. 2019;133(12):1313-1324.

46. Rossbach O, Hung L-H, Schreiner S, et al. Auto- and cross-regulation of the hnRNP L proteins by alternative splicing. *Mol Cell Biol*. 2009;29(6):1442-1451.

47. Martinez FJ, Pratt GA, Van Nostrand EL, et al. Protein-RNA Networks Regulated by Normal and ALS-Associated Mutant HNRNPA2B1 in the Nervous System. *Neuron*. 2016;92(4): 780-795.

48. Ferrero S, Rossi D, Rinaldi A, et al. KMT2D mutations and TP53 disruptions are poor prognostic biomarkers in mantle cell lymphoma receiving high-dose therapy: a FIL study [published online ahead of print 19 September 2019]. *Haematologica*. doi: haematol.2018.214056.

49. Änkö M-L, Müller-McNicoll M, Brandl H, et al. The RNA-binding landscapes of 2 SR proteins reveal unique functions and binding to diverse RNA classes. *Genome Biol*. 2012;13(3):R17.

50. Saltzman AL, Pan Q, Blencowe BJ. Regulation of alternative splicing by the core spliceosomal machinery. *Genes Dev*. 2011;25(4): 373-384.

51. Pereverzev AP, Gurskaya NG, Ermakova GV, et al. Method for quantitative analysis of nonsense-mediated mRNA decay at the single cell level. *Sci Rep*. 2015;5(1):7729.

52. Noensie EN, Dietz HC. A strategy for disease gene identification through nonsense-mediated mRNA decay inhibition. *Nat Biotechnol*. 2001;19(5):434-439.

53. Yang P, Zhang W, Wang J, Liu Y, An R, Jing H. Genomic landscape and prognostic analysis of mantle cell lymphoma. *Cancer Gene Ther*. 2018;25(5-6):129-140.

54. Grünewald TGP, Cidre-Aranaz F, Surdez D, et al. Ewing sarcoma. *Nat Rev Dis Primers*. 2018;4(1):5.

55. Sanchez G, Delattre O, Auboeuf D, Dutertre M. Coupled alteration of transcription and splicing by a single oncogene: boosting the effect on cyclin D1 activity. *Cell Cycle*. 2008; 7(15):2299-2305.

56. Chen H-Y, Yu Y-H, Yen PH. DAZAP1 regulates the splicing of Crem, Crisp2 and Pot1a transcripts. *Nucleic Acids Res*. 2013;41(21): 9858-9869.

57. Honoré B, Baandrup U, Vorum H. Heterogeneous nuclear ribonucleoproteins F and H/H′ show differential expression in normal and selected cancer tissues. *Exp Cell Res*. 2004;294(1):199-209.

58. Rauch J, O'Neill E, Mack B, et al. Heterogeneous nuclear ribonucleoprotein H blocks MST2-mediated apoptosis in cancer cells by regulating A-Raf transcription. *Cancer Res*. 2010;70(4):1679-1688.

59. Sun Y-L, Liu F, Liu F, Zhao X-H. Protein and gene expression characteristics of heterogeneous nuclear ribonucleoprotein H1 in esophageal squamous cell carcinoma. *World J Gastroenterol*. 2016;22(32):7322-7331.

60. Geuens T, Bouhy D, Timmerman V. The hnRNP family: insights into their role in health and disease. *Hum Genet*. 2016;135(8): 851-867.

61. Wang E, Aslanzadeh V, Papa F, Zhu H, de la Grange P, Cambi F. Global profiling of alternative splicing events and gene expression regulated by hnRNPH/F. *PLoS One*. 2012; 7(12):e51266.

62. Änkö M-L, Morales L, Henry I, Beyer A, Neugebauer KM. Global analysis reveals SRp20- and SRp75-specific mRNPs in cycling and neural cells. *Nat Struct Mol Biol*. 2010; 17(8):962-970.

63. Jumaa H, Nielsen PJ. The splicing factor SRp20 modifies splicing of its own mRNA and ASF/SF2 antagonizes this regulation. *EMBO J*. 1997;16(16):5077-5085.

64. Pervouchine D, Popov Y, Berry A, Borsari B, Frankish A, Guigó R. Integrative transcriptomic analysis suggests new autoregulatory splicing events coupled with nonsense-mediated mRNA decay. *Nucleic Acids Res*. 2019;47(10): 5293-5306.

65. Cannell IG, Merrick KA, Morandell S, et al. A Pleiotropic RNA-Binding Protein Controls Distinct Cell Cycle Checkpoints to Drive Resistance of p53-Defective Tumors to Chemotherapy. *Cancer Cell*. 2015;28(5):623-637.

66. Díaz-Muñoz MD, Turner M. Uncovering the Role of RNA-Binding Proteins in Gene Expression in the Immune System. *Front Immunol*. 2018;9:1094.

67. Saha S, Murmu KC, Biswas M, et al. Transcriptomic Analysis Identifies RNA Binding Proteins as Putative Regulators of Myelopoiesis and Leukemia. *Front Oncol*. 2019;9: 692.

68. LeFave CV, Squatrito M, Vorlova S, et al. Splicing factor hnRNPH drives an oncogenic splicing switch in gliomas. *EMBO J*. 2011; 30(19):4084-4097.

69. Golan-Gerstl R, Cohen M, Shilo A, et al. Splicing factor hnRNP A2/B1 regulates tumor suppressor gene splicing and is an oncogenic driver in glioblastoma. *Cancer Res*. 2011; 71(13):4464-4472.

70. Xu C, Xie N, Su Y, et al. HnRNP F/H associate with hTERC and telomerase holoenzyme to modulate telomerase function and promote cell proliferation [published online ahead of print 20 December 2019]. *Cell Death Differ*. 2019;

71. Hong S. RNA Binding Protein as an Emerging Therapeutic Target for Cancer Prevention and Treatment. *J Cancer Prev*. 2017;22(4): 203-210.

72. Quesada V, Conde L, Villamor N, et al. Exome sequencing identifies recurrent mutations of the splicing factor SF3B1 gene in chronic lymphocytic leukemia. *Nat Genet*. 2011;44(1): 47-52.

73. Rossi D, Bruscaggin A, Spina V, et al. Mutations of the SF3B1 splicing factor in chronic lymphocytic leukemia: association

with progression and fludarabine-refractoriness. *Blood*. 2011;118(26):6904-6908.

74. Wang L, Lawrence MS, Wan Y, et al. SF3B1 and other novel cancer genes in chronic lymphocytic leukemia. *N Engl J Med*. 2011;365(26):2497-2506.

75. Wang L, Brooks AN, Fan J, et al. Transcriptomic Characterization of SF3B1 Mutation Reveals Its Pleiotropic Effects in Chronic Lymphocytic Leukemia. *Cancer Cell*. 2016;30(5):750-763.

76. Ten Hacken E, Valentin R, Regis FFD, et al. Splicing modulation sensitizes chronic lymphocytic leukemia cells to venetoclax by remodeling mitochondrial apoptotic dependencies. *JCI Insight*. 2018;3(19):e121438.

77. Te Raa GD, Derks IA, Navrkalova V, et al. The impact of SF3B1 mutations in CLL on the DNA-damage response. *Leukemia*. 2015;29(5):1133-1142.